Electronic Supplementary Material (ESI) for Environmental Science: Water Research & Technology.

Supplementary Information for Energy Recovery in Capacitive Deionization Systems with Inverted Operation Characteristics

Ayokunle Omosebi[a*], Zhiao Li[b], Nicolas Holubowitch[c], Xin Gao[a], James Landon[ad], Aaron Cramer[e], and Kunlei Liu[af*]

[a]Center for Applied Energy Research, University of Kentucky, Lexington KY 40511, USA

[b]Tsinghua University

[c]Department of Physical and Environmental Sciences, Texas A&M University, Corpus Christi, TX

[d]Department of Chemical and Materials Engineering, University of Kentucky, Lexington, KY 40506, USA

[e]Department of Electrical and Computer Engineering, University of Kentucky, Lexington, KY 40506, USA

[f]Department of Mechanical Engineering, University of Kentucky, Lexington, KY 40506, USA

*: *Ayokunle.omosebi@uky.edu*

*: *Kunlei.Liu@uky.edu*

Introduction

In this section, we provide the supporting information indicated in the main text. Specifically, we will provide information on the model in section 1, representations for the converter and electrical

dummy cell boards in section 2, and voltage drop and charging time optimization to reduce energy requirement from the power supply for different R_P and R_S combinations in section 3. In section 4, deconvolution of a current profile based on values for R_P and R_S is shown, and in section 5 Randles circuit fitting to i-CDI and i-MCDI current profiles is shown. In sections 6 and 7, i-CDI and i-MCDI performance data as well as charge storage results during the constant voltage charging of the i-CDI and i-MCDI cells are shown. Finally, in section 8, results from thermodynamic energy efficiency assessment are presented.

1. Model description for recovery system

Model equations are obtained by applying Kirchhoff's voltage (KVL) and current (KCL) laws to circuit loops or nodes in Figure 3. The nodes of interest are numbered 1 through 12. Considering the loop formed by points 2, 3, 11 and 12, the current flowing to the first cell, i_1, can be described by

$$L\frac{di_1}{dt} = V_1 - i_1 * (R_{SR} + R_l) - V_{sw1} \tag{3}$$

Here R_{SR} and R_L are the resistances across sensors and inductors, respectively. V_1 is the voltage sensed between nodes 2 and 12, which is equivalent to the total voltage across cell 1. By similarly considering the loop formed by nodes 6, 7, 9, and 10, the current can be described by

$$L\frac{di_2}{dt} = V_2 - i_2 * (R_{SR} + R_l) - V_{sw2} \tag{4}$$

The voltages across the MOSFET switches SW_1 and SW_2 can be obtained from the loop formed by nodes 3, 6, 10, 11.

$$V_{sw1} = D_1 * i_{sw1} * R_{sw} + (1 - D_1) * \left(V_{cf} - V_{sw2}\right) \tag{5}$$

$$V_{sw2} = (1 - D_1) * i_{sw2} * R_{sw} + D_1 * \left(V_{cf} - V_{sw1}\right) \quad (6)$$

and the respective currents flowing across the switches are obtained from node 11 for i_{sw1} and 10 for i_{sw2}.

$$i_{sw1} = D_1 * (i_1 - i_2) \quad (7)$$

$$i_{sw2} = (1 - D_1) * (i_2 - i_1) \quad (8)$$

The current into the transfer capacitor can be obtained by considering node 3 where

$$C_f \frac{dV_{cf}}{dt} = i_{lf} + i_1 - i_{sw1} \quad (9)$$

By considering loop 3, 4, 5, and 6, the voltage across the transfer capacitor, V_{cf}, can be obtained according to

$$L_f \frac{di_{lf}}{dt} = V_{in} - V_{cf} - R_{lf} * i_{lf} \quad (10)$$

From node 1, the current into cell 1 can be obtained by

$$C \frac{dV_{c1}}{dt} = -i_1 - \frac{Vc_1}{R_p} \quad (11)$$

and from KCL at node 8, the current to cell 2 can be obtained from

$$C \frac{dV_{c2}}{dt} = -i_2 - \frac{Vc_2}{R_p} \quad (12)$$

The six differential equations presented are subject to the following initial conditions:

$$i_{Lf0} = \frac{V_{PS}}{\left(R_s + R_l + R_{lf} + R_{sw} * \frac{R_s + R_l}{R_s + R_l + R_{sw}}\right)} \quad (13)$$

$$i_{10} = -i_{Lf0} \quad (14)$$

$$i_{20} = -R_{sw} * \frac{i_{L10}}{R_{sw} + R_s + R_l} \tag{15}$$

$$V_{Cf0} = V_{PS} - i_{Lf0} * R_f \tag{16}$$

$$V_{C10} = 0 \tag{17}$$

$$V_{C20} = 0 \tag{18}$$

The electronic circuit for the cells and converter, including their corresponding differential equations and initial conditions were converted to a MATLAB Simulink™ model, and their solution was obtained using the ordinary differential equation package ODE23TB.

2. Converter and Electrical Dummy Cell

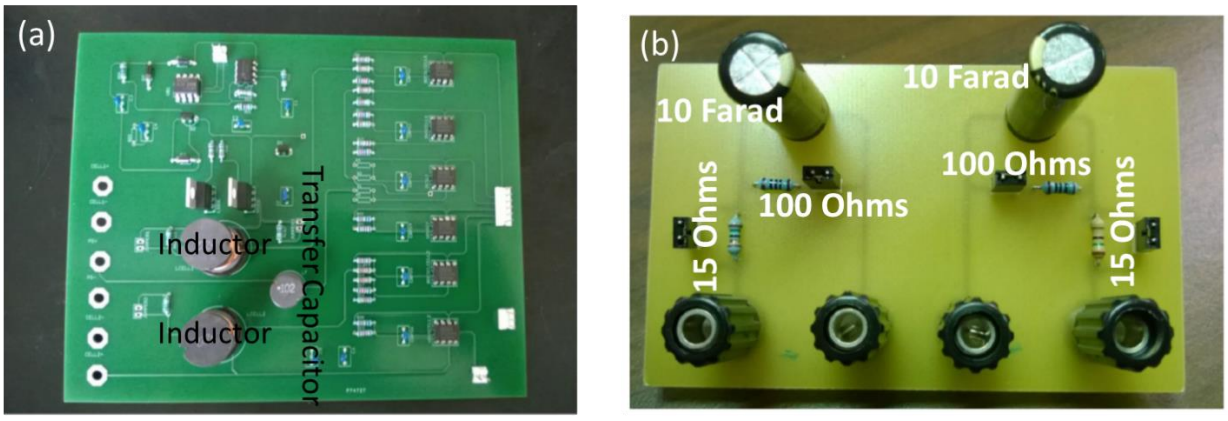

Figure S1. Pictures of (a) converter and (b) electrical dummy cell boards.

3. Impact of R_S and R_P on Energy Recovery

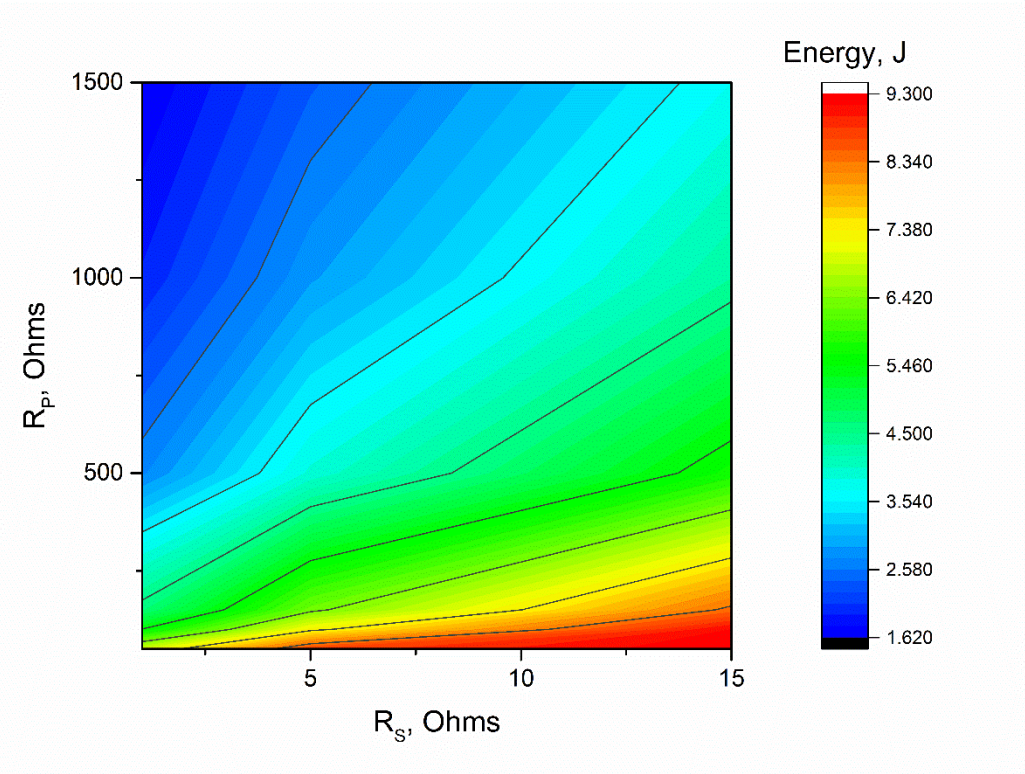

Figure S2. Impact of the parallel (R_P) and serial (R_S) resistors on the energy input requirement of the power supply.

Table S1. Voltage drop and charging time optimization for R_P and R_S combinations.

Rs Ohms \ RP	50	100	150	500	1000	1500
1	0.24 V 180s (6.9827 J)	0.24v 240s (5.4722)	0.12v 300s (4.636)	0.12v 480s (2.7098)	0.12v 720s (1.9645)	0.12v 840s (1.6255)
5	0.36v 240s (8.7171)	0.24v 360s (7.2855)	0.24v 420s (6.3312)	0.12v 780s (3.9012)	0.12v 1080s (2.8692)	0.12v 1320s (2.3879)
15	0.36v 300s (9.2923)	0.36v 480s (9.1457)	0.24v 600s (8.4184)	0.24v 1140s (5.6863)	0.12v 1740s (4.3358)	0.12v 1800s (3.7011)
150	0.72v 180s (1.1794)	0.72v 660s (4.1722)	0.72v 960s (6.376)	0.36v 1800s (9.8122)	0.36v 1800s (8.9386)	0.36v 1800s (8.6232)
1000	0.24v 60s (0.05422)	0.24v 60s (0.053744)	0.24v 60s (0.053531)	0.36v 1800s (2.9079)	0.36v 1800s (2.8656)	0.36v 1800s (2.85)

4. .Deconvolution and response of current to R_P and R_S.

Equations describing circuit in Figure S3a are depicted below.

$$V_C = \frac{R_P V_{PS}}{R_S + R_P}\left(1 - \exp\left(-t\frac{R_S + R_P}{C R_S R_P}\right)\right) \quad (s1)$$

$$i_C = \frac{V_{PS}}{R_S}\exp\exp\left(-t\frac{R_S + R_P}{C R_S R_P}\right) \quad (s2)$$

$$i_P = \frac{V_C}{R_P} \quad (s3)$$

$$i = i_C + i_P \quad (s4)$$

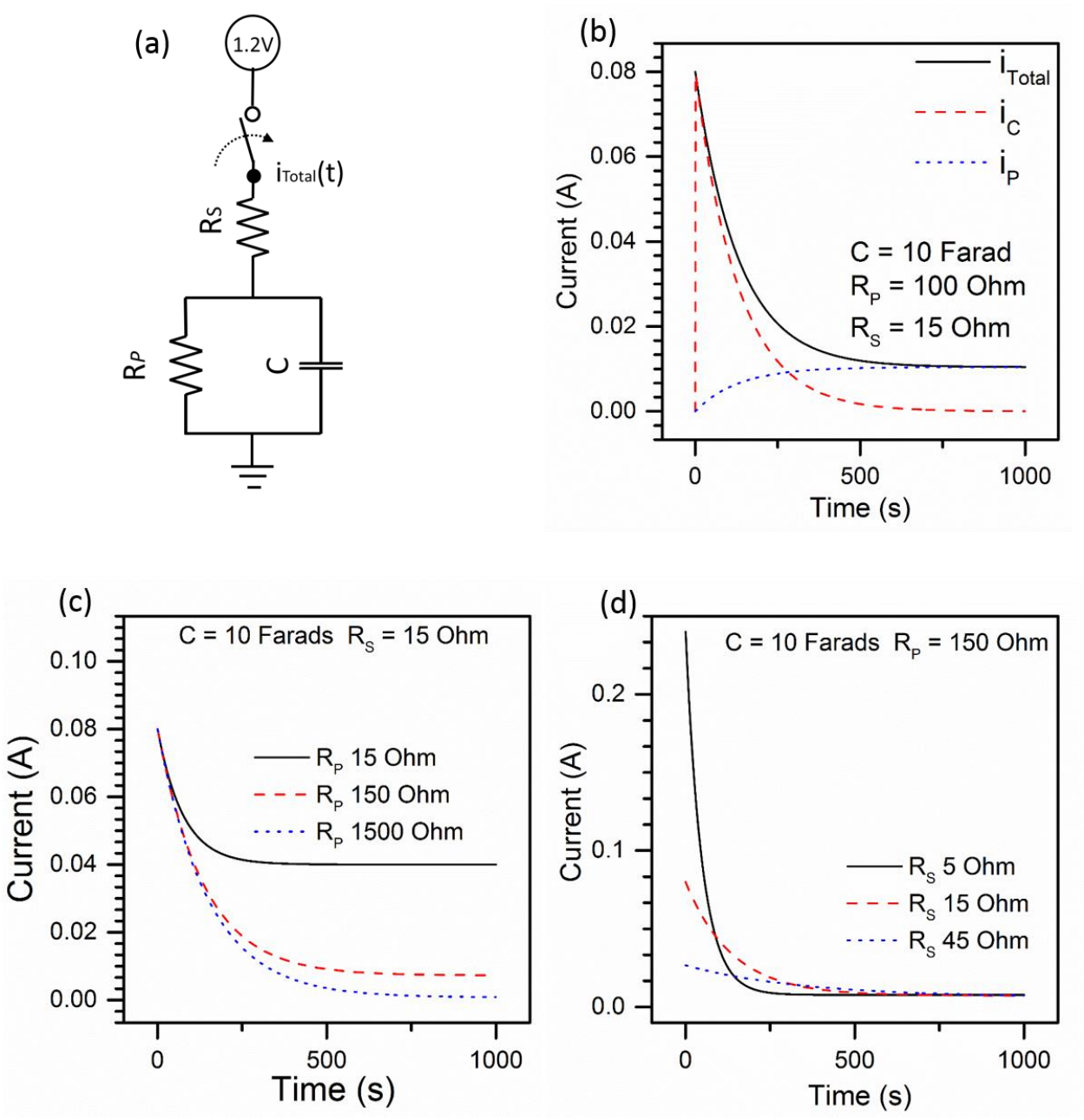

Figure S3. Deconvolution and response of current to R_P and R_S.

5. Randles fitting results for iCDI and iMCDI current profiles

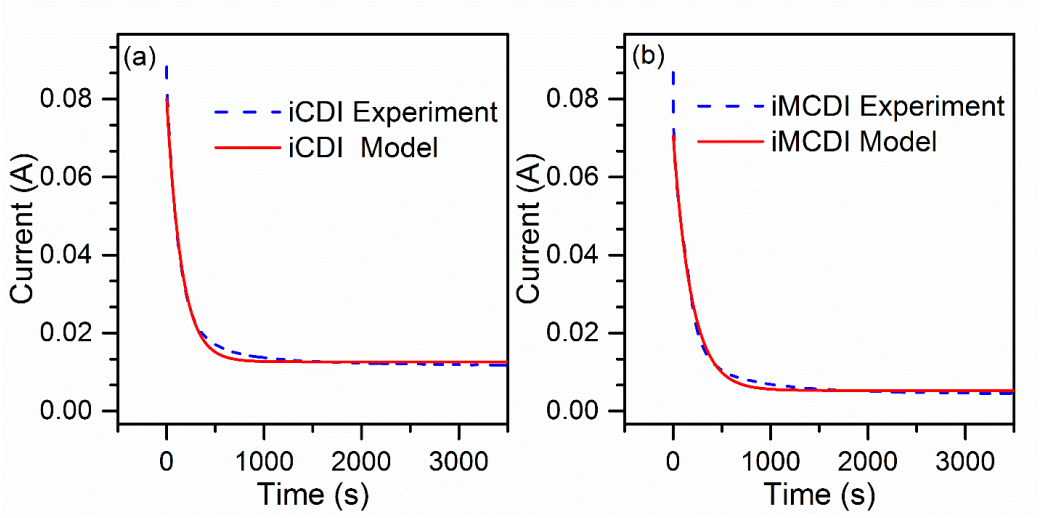

Figure S4. Randles circuit fitting results for iCDI (a) and iMCDI (b) current profiles. The C, R_S, and R_P values were 12 F, 15 Ohms, and 80 Ohms for the iCDI cell, and 12 F, 17 Ohms, and 210 Ohms for the iMCDI cell.

6. Performance of i-CDI and i-MCDI cells

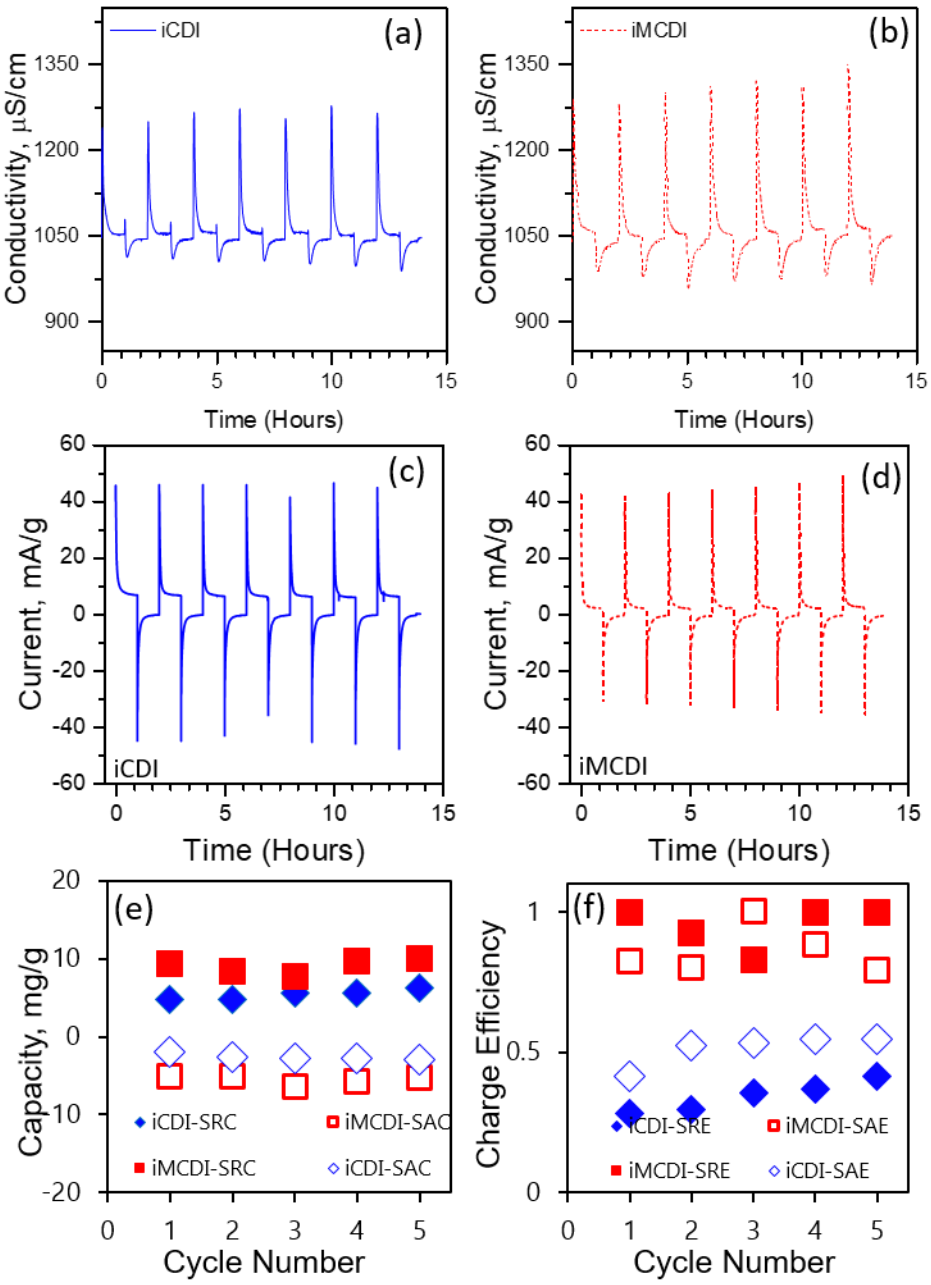

Figure S5. Conductivity profiles (a-b) and current response (c-d), salt regeneration (SRC) and salt adsorption (SAC) capacities (e), and charge efficiency (f) during cycling of i-CDI and i-MCDI cells at 1.2/0 V.

7. Ion charge storage in i-CDI and i-MCDI cells

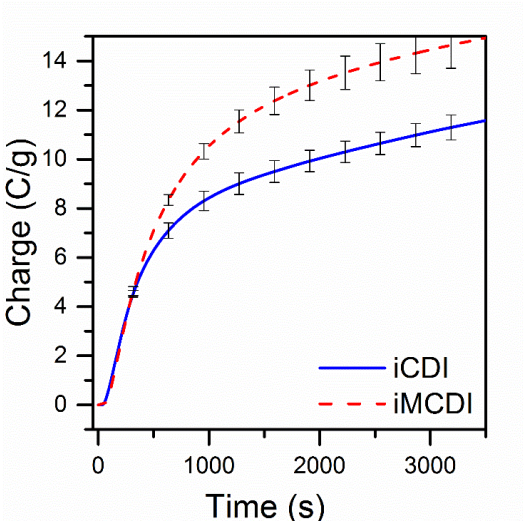

Figure S6. Ionic charge passed during charging of the iCDI and iMCDI cells at a constant voltage of 1.2 V.

8. Thermodynamic Energy Efficiency of i-CDI and i-MCDI cells with and without energy recovery

Table S1. Thermodynamic efficiency of i-CDI and i-MCDI cells with and without energy recovery for storing 6 C/g of ionic charge from a 10 mM NaCl influent stream at 14 ml/min assuming a water recovery of 50%

Mode	Electrode (g)	Energy Consumed (J)	Energy Consumed (kWh/m³)	ΔG (kWh/m³)	TEE	Delta Time for 6 C/g (seconds)
iCDI	1.9	21.6	0.043	9.46468E-05	0.002	611
iCDI -Recovery	1.9	14.6	0.017	3.34103E-05	0.002	1028
i-MCDI	2.1	17.1	0.040	0.000164797	0.004	512
i-MCDI- Recovery	2.1	8.5	0.016	0.000104087	0.007	644